V European Conference on Computational Fluid Dynamics
ECCOMAS CFD 2010
J. C. F. Pereira and A. Sequeira (Eds)
Lisbon, Portugal, 14–17 June 2010

COMPARISONS OF WAVE OVERTOPPING AT COASTAL STRUCTURES CALCULATED WITH AMAZON, COBRAS-UC AND SPHYSICS

M.G. Neves*, M.T. Reis*, E. Didier*†

* Laboratório Nacional de Engenharia Civil
Av. do Brasil, 101, 1700-066 Lisbon, Portugal
e-mail: gneves@lnec.pt, treis@lnec.pt, edidier@lnec.pt

† MARETEC
IST, Av. Rovisco Pais, 1049-001, Lisbon, Portugal

Key words: Coastal structures, Wave overtopping, NLSW model, RANS model, SPH model

Abstract. *The use of numerical models to calculate the mean overtopping discharges is, nowadays, more frequent in preliminary design of coastal structures, since they are more flexible than both empirical/semi-empirical and physical models and, once calibrated and validated, they can be applied reliably to a large range of alternative structure geometries and wave conditions. There are different models that can be used to calculate the mean overtopping discharges over a structure. The paper compares the output from three numerical models used to predict the mean overtopping discharges: AMAZON [1], based on solving the non-linear shallow-water equations; and two models based on Reynolds averaged Navier-Stokes equations, COBRAS-UC [2], a Eulerian model using the volume of fluid (VoF) method for surface capturing, and SPHysics [3], a Lagrangian model based on Smoothed Particle Hydrodynamics (SPH). The numerical results are also compared with experimental data obtained at the National Civil Engineering Laboratory (LNEC), Portugal, in the framework of the Composite Modelling of the Interactions between Beaches and Structures (CoMIBBs) project, a joint research activity of the HYDRALAB III European project [4]. The experimental work consists of wave propagation, with breaking, and wave overtopping of an impermeable seawall, a common coastal defense structure employed at the Portuguese coast.*

Results of free-surface elevation along the computational domain and of mean overtopping discharges are presented and discussed. Although the processes of wave generation used in the laboratory and in the models were different, the agreement in the free surface was reasonable: the wave period obtained with the models agreed very well with the data and the shape of the wave presented some minor differences to the physical model data, as well as the wave height. The results of mean overtopping discharges obtained with the three models agreed very well with the physical model results.

1 INTRODUCTION

Wave overtopping is one of the most difficult phenomena of wave-structure interaction to reproduce accurately both physically and numerically. In the case of an impermeable coastal defense where breaking occurs, a good simulation of the overtopping demands a correct representation of all phenomena involved, including reflection on the structure, breaking, non-linear wave interaction, run-up, etc.

The use of numerical models to calculate the mean overtopping discharges is, nowadays, more frequent in preliminary design of coastal structures, since they are more flexible than both empirical/semi-empirical and physical models and, once calibrated and validated, they can be applied reliably to a large range of alternative structure geometries and wave conditions. Different models have been applied in several case studies as the volume of fluid (VoF) method [5, 6, 7], surface capturing (SC) approach [8, 9] and smoothed particle hydrodynamics (SPH) models [10]. Each kind of model has its advantages and limitations. Their use in practical engineering applications is limited by their computational efficiency, their need for calibration, the possibility of representation of certain structural characteristics, among others.

This paper compares results from different models to compute the mean wave overtopping discharge for a schematic coastal defense tested at the National Civil Engineering Laboratory (LNEC), Portugal, in the framework of the Composite Modelling of the Interactions between Beaches and Structures (CoMIBBs) project, a joint research activity of the HYDRALAB III European project [4]. The experimental work, carried out using a 1:10 geometrical scale, consists of wave propagation, with breaking, and wave overtopping of an impermeable seawall, representing a coastal defense structure employed at the Portuguese coast.

The models used are: AMAZON [11], based on solving the non-linear shallow-water (NLSW) equations, COBRAS-UC [2, 7], a Eulerian model using the volume of fluid (VoF) method for surface capturing, and SPHysics [3, 12], a Lagrangian model based on Smoothed Particle Hydrodynamics (SPH).

AMAZON has been validated and extensively used to study the random wave overtopping of dikes. One of the prime virtues of this kind of numerical model lies in its speed of calculation. Some of the disadvantages are that the wave conditions have to be input at a distance from the structure toe of approximately one wavelength [13] and satisfy the shallow water restriction and, since it is a depth-integrated model, the velocity profile and the pressure at the structure cannot be obtained. COBRAS-UC has been validated for random waves acting on submerged, permeable structures at both model and prototype scales. It can simulate all of the important hydrodynamic processes involved in wave overtopping of permeable complex structures. The main disadvantages are related with the time it takes to run and the need for calibration of the porous flow. SPHysics has been used for several applications [3, 12, 14, 15] and validated for regular wave and overtopping of impermeable structures. The Lagrangian technique allows simulating complex free surface flows, like dam-break, wave breaking and overtopping. However, it is especially time-consuming.

Following this introduction, a description of the models is presented in section 2. Section 3 briefly describes the case study, the physical model test used here and the application of the models to this case study. Section 4 presents the results of free-surface elevation along the computational domain and of mean overtopping discharges at the structure obtained with the models, and compares those results with the experimental data. The paper ends with some main conclusions.

2 MATHEMATICAL MODELS

2.1 AMAZON

AMAZON was originally developed at Manchester Metropolitan University [11], it is written in C++ and it comes as both a one-dimensional model, applied here, and as a two-dimensional plan model. It is based on solving the non-linear shallow-water (NLSW) equations, which are a simplification of the Reynolds equations by depth integration. It simulates random waves and wave breaking is approximated by steep fronts represented by bores. AMAZON uses a “non-reflective wave inlet boundary condition", which is able to remove at the seaward boundary more than 98% of the energy of any waves reflected from the modeled structures. As a consequence, the seaward boundary can be set close to the structure to avoid deep water conditions, where AMAZON has limitations. It is capable of generating grid cells with any shape and varying dimensions. The output defines the free surface, depth-averaged velocities and, based on these values, discharge time-series, mean discharge and peak discharge at two locations on the structure.

AMAZON has been validated for a variety of representative test problems [11] involving steady and unsteady, inviscid and viscous, and subcritical and supercritical flows. It has also been validated and extensively used to study the wave overtopping of impermeable dikes. However, AMAZON has not been systematically validated to study the overtopping of porous structures yet, since its original version did not explicitly account for porous flow. The development and initial validation of the porous flow model has been carried out only recently [1, 16, 17, 18]. To govern the water exchange between the porous cells, both the Darcy and the Forchheimer equations are implemented.

In spite of AMAZON limitations, mainly relating to the shallow water assumptions, it is already being used for the purposes of design and flood forecasting, since wave trains of several thousand random waves are simulated rapidly.

A detailed description of AMAZON can be found in Hu [11] and in Reis et al. [1, 16].

In this study, AMAZON was applied to calculate the surface elevation and the mean wave overtopping discharge for a coastal structure, which is basically an impermeable slope.

2.2 COBRAS-UC

By taking the volume-average of RANS equations, Lin and Liu [19] presented a two-dimensional numerical model, nicknamed COBRAS, to describe the flow inside and outside coastal structures including permeable layers. Hsu et al. [5] extended the preliminary model by including a set of volume-averaged k-ε turbulence balance equations. The movement of free surface is tracked by the Volume of Fluid (VOF) method.

COBRAS-UC is a new version of the model developed at the University of Cantabria to overcome some of the initial limitations and especially to convert it into a tool for practical application. Most of these modifications have been based on the extensive validation work carried out with the model for low-crested structures and for wave breaking on permeable slopes [20, 7]. The improvements cover the wave generation process and code updating; optimization and improvement of the main subroutines; improvement of input and output data definition and the development of a graphical user interface and output data processing programs.

In this study, COBRAS-UC was used to calculate the surface elevation and the mean wave overtopping discharge for the coastal structure mentioned in section 2.1.

2.3 SPHysics

SPH method was first developed and applied for astrophysics [21, 22], and later for hydrodynamic simulations [23] and coastal applications [24].

SPH approach is completely different from the Eulerian approach, i.e. grid models. The SPH approach is based on mesh-free technique particle method, purely Lagrangian, for modeling fluid flows and facilitates the simulation of problems that require the ability to treat large deformations of free surface flows, complex geometries, nonlinear phenomena and discontinuity. With this approach, moving boundaries, such as a piston wave-maker or moving bodies, are easily implemented. Mesh-free particle methods treat the system as a set of particles that represents small volume of water, for hydrodynamic applications. So, for Computational Fluid Dynamics (CFD), variables transported by the particles, such as mass, position, velocity, density and pressure, are computed for each particle.

In this study, SPHysics (SPHysics code, [25]) was applied to model wave propagation and overtopping of the impermeable coastal structure mentioned in section 2.1. SPHysics model is an open-source SPH solver inspired by the formulation of Monaghan [26] and developed jointly by a group of researchers of various universities [3]. The fluid in the standard SPH formalism is treated as weakly compressible. The model presents a modular form and a variety of features are available to choose different options: 2D and 3D model; time schemes: predictor-corrector or Verlet algorithm; constant or variable time step; various kernels (interpolation functions); viscosity models: artificial, laminar and sub-particle scale turbulence model; density re-initialization: Shepard or MLS; solid boundary conditions: dynamic boundaries, repulsive forces, periodic open boundaries; etc.

3 CASE STUDY

The numerical results are compared with experimental data collected at the National Civil Engineering Laboratory (LNEC), Portugal, in the framework of the *Composite Modelling of the Interactions between Beaches and Structures (CoMIBBs)* project, a joint research activity of the HYDRALAB III European project [4]. The experimental work used in this paper was carried out using a 1:10 geometrical scale and consists of wave propagation, with breaking, and wave overtopping of an impermeable seawall, a common coastal defense structure employed at the Portuguese coast [27].

The structure is a hypothetical sea defense sited at São Pedro do Estoril, located on the west coast of Portugal (Figure 1). It comprises a seawall with a 1:1.5 slope fronted by a 1:20 beach foreshore (Figure 2).

The general wave regime of the west coast of Portugal is broadly characterized by significant wave heights, H_s, varying from 1 m to 6 m and peak wave periods, T_p, from 8 s to 14 s.

Figure 1: Location, aerial view and photograph of São Pedro do Estoril.

In the experimental work used in this paper, wave propagation started 357.4 m before the toe of the foreshore, at a horizontal seabed located 10 m below chart datum (CD) (Figure 2). A tidal level of +1.5 m CD was considered together with a wave condition characterized by regular waves of height H=4 m and period T=12 s, in prototype dimensions.

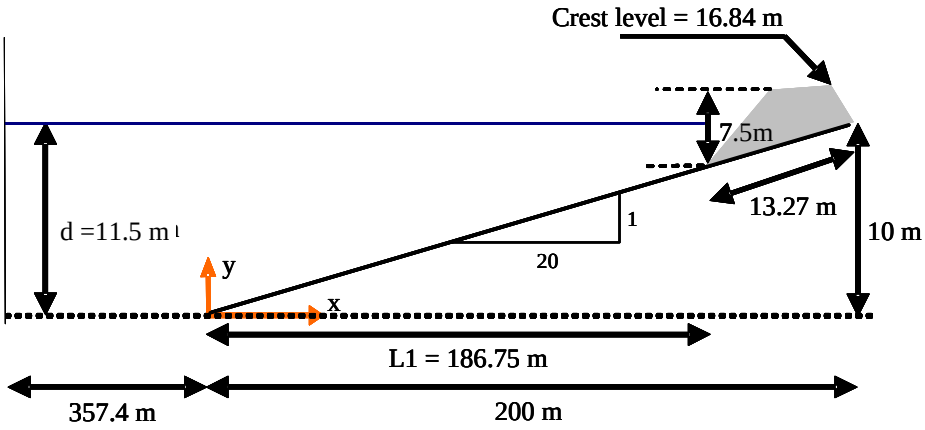

Figure 2: Schematic representation of the prototype cross-section and the coordinate system.

3.1 Physical model test

The physical model test used in this paper was carried out with regular waves in one flume at LNEC (Figure 3), which is approximately 73 m long, 3 m wide, has an operating water depth of 2 m and is equipped with a piston-type wave-maker and an active wave absorption system, AWASYS [28], which allows the absorption of reflected waves.

Figure 3: Overview of wave flume and model structure.

The physical model was built and operated according to Froude's similarity law, using a geometrical scale of 1:10 and it was built to reproduce the prototype cross-section shown in Fig. 2. The model structure was impermeable, made of wood and it had a 1:1.5 front slope with small blocks attached to it, to simulate roughness (Figure 4). The seabed in front of the model structure was represented by a ramp with a 1:20 impermeable slope, followed by a horizontal bottom.

Figure 4: Equipment used and overview of wave overtopping.

To determine the free-surface elevation, the flume was equipped with six resistive-type wave gauges (Figure 4). A fixed array of two gauges, located in front of the wave-maker, was needed for the dynamic wave absorption system. A moveable array of four gauges was used to characterize the free-surface elevation along the flume.

To measure induced pressures at the structure, four pressure transducers were placed on the structure (Figure 4). A resistive type wave gauge was located 3 mm above the face of the model structure to determine run-up levels (Figure 4).

A tank with a triangular weir on one of its sides was located at the back of the structure to collect the water overtopping the structure (Figure 4). The water was conducted to the tank by means of a chute, 50 cm wide. A water-level gauge was used inside the tank to measure the variation in water level within a test run.

A computer collected and stored the data in digital format at a frequency of 50 Hz.

Tests with regular waves lasted for 5 minutes and for each wave condition, the test was repeated at least six times, each with the moveable array in a different position, in order to have the surface elevation measured at twenty four different locations along the flume.

Figure 5 presents the mean overtopping discharges obtained from the physical model for the test conditions considered in this study, corresponding to a wave height H=0.40 m and a wave period T=3.79 s for a water depth close to the wave maker h=1.15 m.

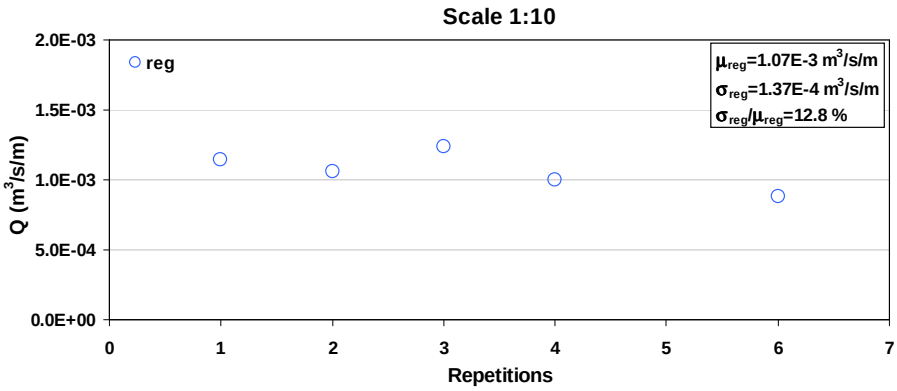

Figure 5: Mean overtopping discharge, Q, obtained with physical model for the test conditions considered in this study.

The figure also shows the means, μ, standard deviations, σ, and coefficients of variation, σ/μ, of the discharges. For this case, breaking occurs around x=8.5 m (x=0 m at the toe of the foreshore). After that, due to interaction between the incident and the reflected waves, a maximum value of the surface elevation is reached for x around 11 m.

3.2 AMAZON

The physical model location, dimensions and geometrical characteristics of the foreshore and of the structure were reproduced within AMAZON. Five sections were considered in the model: 4 were located at the same positions as the 4 wave gauges in the physical model (x=9.5 m, 10.0 m, 10.5 m and 11.0 m) and one was positioned on top of the structure to compute the overtopping discharge.

AMAZON's landward boundary was a full absorption boundary set 0.20 m behind the crest of the wall. According to Hu and Meyer [13], AMAZON produces good results when its seaward boundary is located at a distance from the structure toe of approximately one wavelength, L_s, where L_s is the shallow water wavelength in depth d_s at the structure toe, calculated using the peak period of the incident waves, T_p ($L_s = T_p(gd_s)^{0.5}$ in which g is the acceleration due to gravity). In this study, d_s=0.216 m and T_p=3.79 s, which gives L_s=5.52 m, i.e. according to Hu and Meyer [13], the seaward boundary should be located at x=13.16 m. However, as mentioned above, at this location wave breaking has already occurred and at about x=11 m there was a considerable increase of the surface elevation due to interaction between the incident and the reflected waves. Furthermore, during the physical model tests, there was no gauge located at approximately this position. Consequently, sensitivity tests were carried out with different positions to establish what effect the location of the seaward boundary had on AMAZON's overtopping predictions (Table 1). Different input wave series were used: from the physical model tests, from COBRAS-UC and from SPHysics, all representing the incident plus the reflected waves (measured series). Since AMAZON is a depth-averaged model, i.e. the velocities of the incident and reflected waves are not introduced as input to the model, the incident wave series should be used, instead of the measured series, but the experimental data required for separating the incident and the reflected waves were not available.

x (m)	d (m)	d/L_{op}	Computational domain (m)	Number of cells (intermediate mesh)
0.0	1.15	0.051	20.0	3046
4.0	0.95	0.042	16.0	2646
5.0	0.90	0.040	15.0	2546
7.5	0.78	0.035	12.5	2296
8.0	0.75	0.033	12.0	2246
8.5	0.73	0.032	11.5	2196
9.0	0.70	0.031	11.0	2146
9.5	0.68	0.030	10.5	2096
10.0	0.65	0.029	10.0	2046
10.5	0.63	0.028	9.5	1996
11.0	0.60	0.027	9.0	1946
12.0	0.55	0.025	8.0	1846

Table 1 – Characteristics of AMAZON runs

The length of the total computational domain varied between 8 m and 20 m with the location of the seaward boundary, as well as the total number of cells, which varied between 1846 and 3046 (Table 1).

The values of the relative water depth, d/L_{op}, at AMAZON's seaward boundary ranged from 0.025 to 0.051 (Table 1), in which L_{op} is the deep water wavelength corresponding to the peak of the incident wave spectrum and calculated, according to linear wave theory, as $L_{op} = gT_{op}^2/(2\pi)$. Researchers have reported different maximum permissible values of d/L_{op} which were found to provide good results when used with the NLSW equations: they varied from 0.016 to 0.19, approximately [29].

Figure 6 shows the mean overtopping discharges obtained with different locations of the seaward boundary for input wave series (incident plus reflected waves) from the physical model tests, from COBRAS-UC and from SPHysics. The two horizontal lines represent values of Q associated with the range of mean discharges obtained in the physical model (see Figure 5).

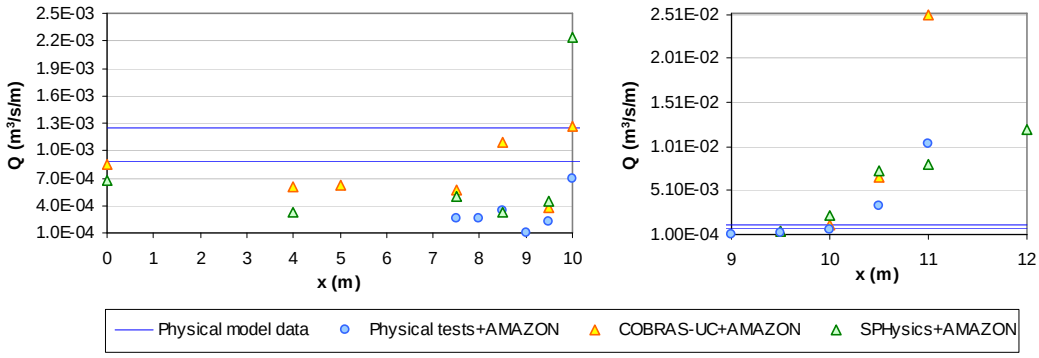

Figure 6: Mean overtopping discharge, Q, obtained using different locations of the seaward boundary for input wave series from the physical model tests, from COBRAS-UC and from SPHysics.

The figure shows that the location of the seaward boundary has a great impact on the results. The general trend is similar for all input wave series, although the input condition for the physical tests is a paddle with an absorption system, for COBRAS-UC is a numerical paddle with an absorption system and for SPHysics it is a numerical paddle without absorption. These different characteristics and the fact that measured wave series are used as input to AMAZON instead of incident wave series, explain the differences in Q between them. Some of the differences between the AMAZON results and the range of Q obtained in the physical model may also be due to the fact that incident wave series alone could not be used (instead of incident plus reflected series).

For $x \leq 9.5$ m, Q oscillates around a mean value of 6.8E-4 $m^3/s/m$ for "COBRAS-UC+AMAZON" and of 4.6E-4 $m^3/s/m$ for "SPHysics+AMAZON", with coefficients of variation of about 37% and 31%, respectively. The mean discharges are generally below the range of Q from the physical model tests. However, for $x>9.5$ m, the trend changes to a monotonic increase of Q with x, reaching a maximum value around 11 m<x<12 m, where a maximum value of the surface elevation is reached due to interaction between the incident and the reflected waves. In this area, where the water depth is small, the velocities of the incident and reflected waves are especially relevant for the wave propagation afterwards and they are not introduced as input to AMAZON, since it is a depth-averaged model. This explains the different trend observed after x=9.5 m and the fact that the obtained discharges are generally considerably above the range of Q from the physical model tests. Consequently, it was decided to locate the seaward boundary before x=9.5 m, at x=8.5 m.

To study the sensitivity of the AMAZON predictions of Q to the mesh refinement, three different grids were tested with the seaward boundary located at x=0 m and using the measured wave series from COBRAS-UC (Table 2), all cases with a non-uniform computation grid.

	Mesh dimension (m)		
Location	**Fine**	**Intermediate**	**Coarse**
Foreshore	0.005	0.01	0.01
Structure	0.001	0.001	0.005
Behind the structure	0.01	0.05	0.05

Table 2 – Characteristics of AMAZON grids

Figure 7 shows the mean overtopping discharges obtained with the different mesh refinements. It shows that the relative difference in discharges between the fine and the coarse grids ($|Q_{fine}-Q_{coarse}|/Q_{fine}$) is 7.4% whereas the relative difference between the fine and the intermediate grids is 0.3%. Based on a compromise between the time AMAZON required for each run and the relative difference in discharges between the grids, it was decided to apply the intermediate grid for all the AMAZON runs (including the ones shown in Figure 6). Note that the numerical tests, which corresponded to 100 s simulations, were all run on an Intel(R) Core(TM)2 Quad CPU Q6600 @2.40GHz with 3.00GB of RAM.

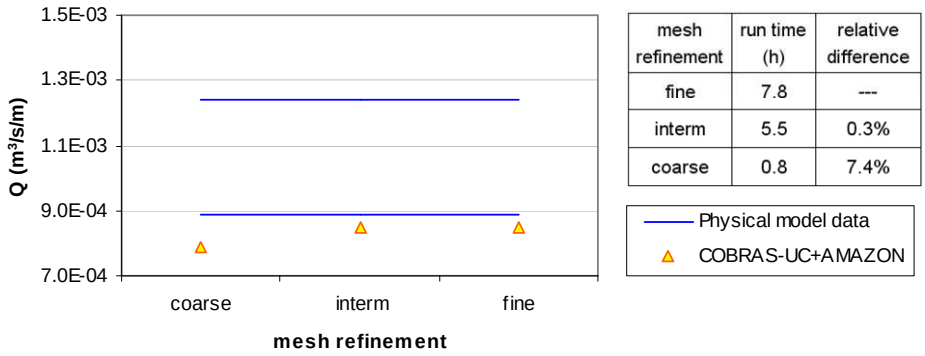

Figure 7: Mean overtopping discharge, Q, obtained using different mesh refinements with the seaward boundary located at x=0 m and using the incident wave series from COBRAS-UC.

The minimum water depth at each cell was set to $2x10^{-5}$ cm. Any cell with a water depth below this minimum value was treated as dry and was excluded from the computation. The minimum value was sufficiently small to represent a dry bed; a smaller value would have resulted in more computational effort for little gain.

3.3 COBRAS-UC

The domain that reproduced the full dimensions of the experimental flume (Figure 8) was 59 m long and 3 m high. The incident wave generation was located at the same distance from the structure as the paddle (piston type) in the flume and it was simulated with a paddle with dynamic absorption. The location, dimensions and characteristics of the experimental structure were reproduced in the computational domain. Twelve sections were considered in the numerical flume: 6 were located at the same positions as the wave gauges in the physical model; one was positioned in the paddle, in order to control the wave generation; two were located at the same positions as the pressure sensors in the physical model; and another three were placed on top of the structure, to compute the overtopping discharge.

In order to make the runs quick in the area dominated by the wave propagation and to refine the grid in the area of interest, a coupling methodology was applied. In this connection, the total domain was divided into two different domains: the first part corresponds to the area dominated by the wave propagation; the second, located as close to the structure as possible, corresponds to the area where the wave-structure interaction is important. Figure 8 shows a schematic representation of the coupling domains.

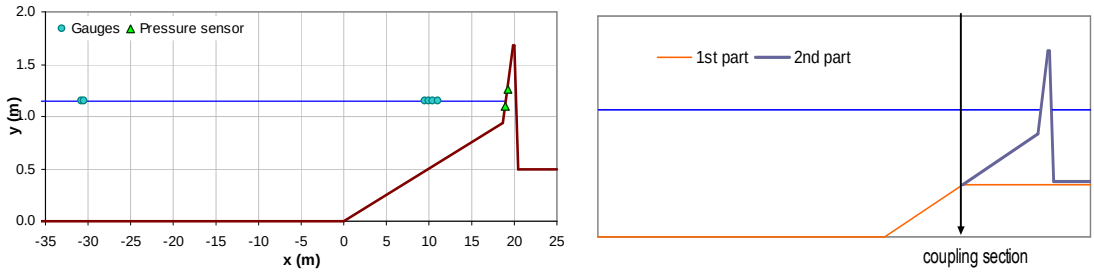

Figure 8: Schematic representation of the domain simulated with COBRAS-UC and position of instruments on the physical model (left) and schematic representation of the coupling domains used (right).

To guarantee the accuracy of the coupling methodology, a sensitivity study of the impact of some coupling characteristics on the results was made previously. The results of the surface elevation and of the mean overtopping discharges obtained by coupling the two parts of the domain were compared with the results obtained when considering one domain for the total flume simulation, using the same regular grid, with a cell width of dx=0.03 m and dy=0.02 m in the x and the y directions, respectively.

The first domain included the area between the paddle and the coupling section and an additional area with a sponge layer, in order to have the waves on the coupling section with no influence of this area. Tests were made with different sponge layer dimension (L, 2L and 4L) and position (2dx, L and 2L from the coupling section). It was concluded that the sponge layer should be at least 2L and could be located very close to the coupling section with no significant errors on the results.

To have an idea of the influence on the results of the coupling section location, four different positions were tested:

- at the ramp (x=7.5 m);
- at the beginning of the ramp (x=0 m);
- at L/2 before the ramp (x=-6 m);
- at L before the ramp (x=-12 m).

The results present some minor differences for the cases where the coupling section was located before the ramp. However, for the coupling section located at the ramp, the differences in the wave height and in the shape of the wave increase. When the analysis is carried out for points that distant more than L from the coupling section the errors obtained in the wave height are, in all cases, less than 10%. However, for points that distant less than L, the absolute value of the relative error between the wave height obtained with coupling grids, H, and with the total flume simulation, $H_{x=-37.5}$, increases up to about 20% (Figure 9). In what concerns the mean overtopping discharge, the same pattern is found: the absolute value of the relative error between the mean overtopping discharge obtained with coupling grids, Q, and with the total flume simulation, $Q_{x=-37.5}$, decreases with the increase of the distance of the coupling section to the structure, as can be seen in Figure 9.

To illustrate the results obtained, Figure 10 presents a detail of the surface elevation at two sections, 10.5 m and 18.9 m, for the different positions of the coupling section (x=7.5 m, 0 m, -6 m and -12 m) and for the total flume (x=-35.7m). The last section

(18.9 m) is the position of the pressure sensor located above the mean water level (see Figure 8), where the waves have already broken.

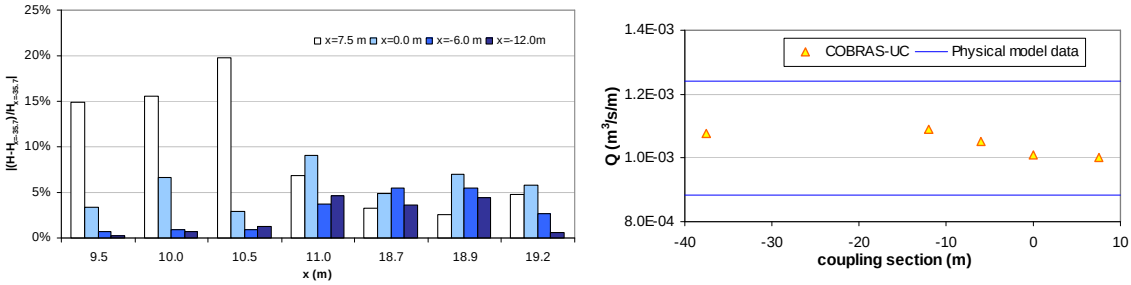

Figure 9: Wave height (left) and mean overtopping discharge (right) relative error associated with coupling section.

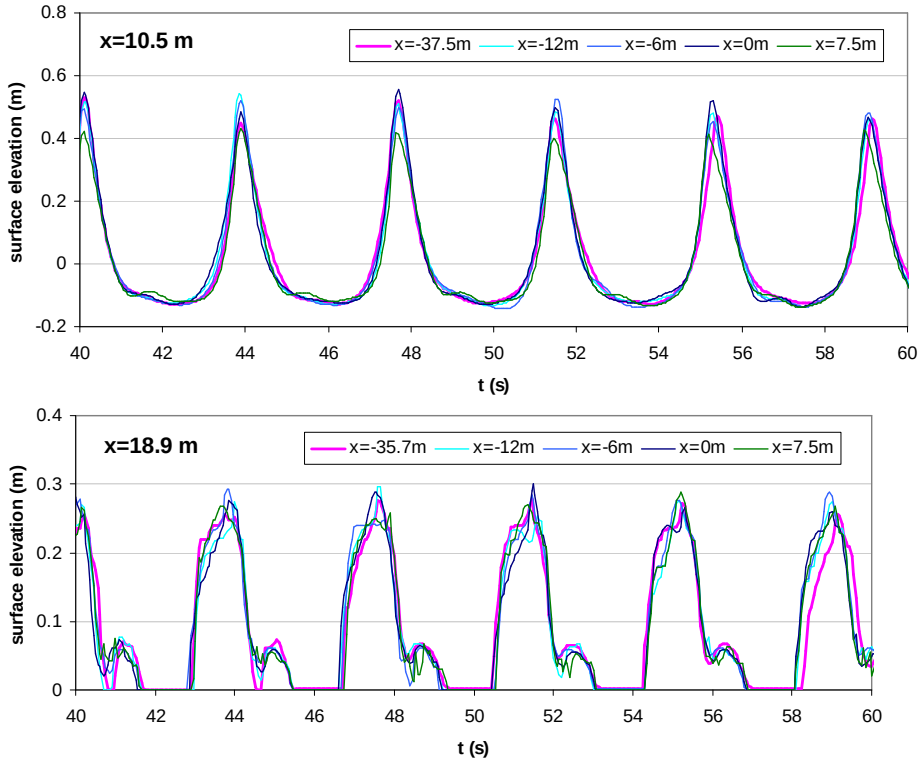

Figure 10: Time series of surface elevation using different coupling section positions and using the total flume (x=-37.5m).

The results obtained suggest that the coupling section should be located at least at L before the area of interest: for the overtopping discharge, the smallest domain could be used (x=7.5 m) since the overtopping occurs at a distance larger than L; for the surface elevation, the gauges used in the physical model tests are located to a distance from the coupling section less than L and the coupling section at x=0 m should be used. Consequently, it was decided to use the two positions of the coupling section (x=0 m and x=7.5 m). For these two second parts of the domain, the computational mesh was refined with minimum cell dimensions of 0.01 m both in the x and the y directions for the case with a coupling section at x=7.5 m and 0.012 m and 0.01 m, respectively, for the coupling section at x=0 m.

Figure 11 compares the results of the surface elevation with a coarse mesh and with a fine mesh obtained for the coupling section located at x=0 m. The results present some minor differences at 10.5 m and some differences in shape and wave height at 18.9 m.

When the analysis is done for the surface elevation on the top of the structure (19.9 m), the differences are relevant, with a large number of waves overtopping the structure for the fine mesh and a mean overtopping discharge increasing around 15% when the mesh in the structure is reduced from 3.0 cm to 1.2 cm. This illustrates the importance of the mesh dimensions when the overtopping discharges are the main goal of the numerical simulations. The same trends are found for the coupling section located at x=7.5 m.

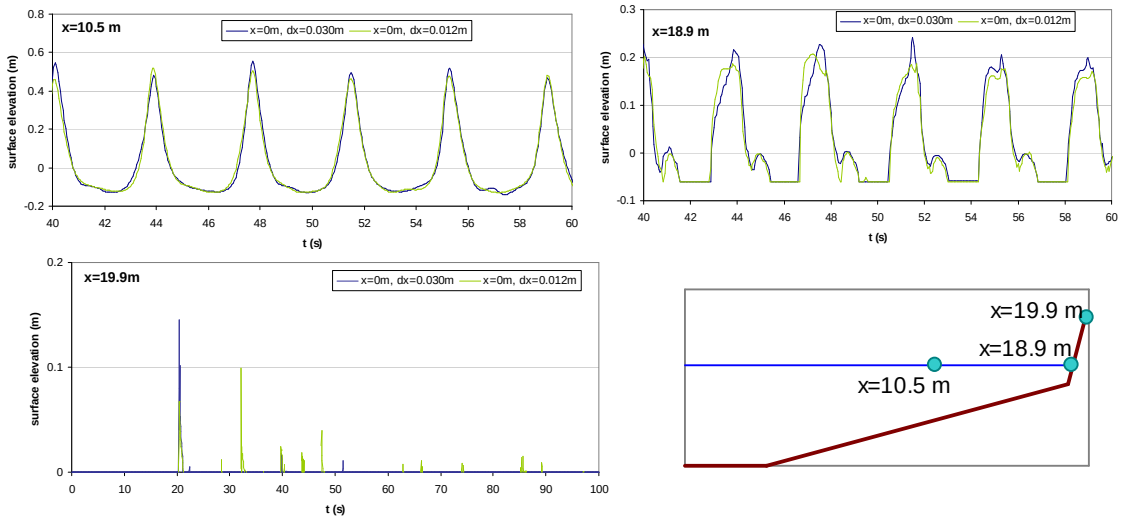

Figure 11: Time series of surface elevation at three different locations for the coupling section at x=0 m and schematic representation of the locations.

Based on the results described before, the meshes that are used in section 4 of this paper correspond to the two fine meshes with locations of the coupling section at x=0 m and x=7.5 m. These computational meshes were divided in two regions of different resolutions (Figure 12): between the generation zone and the structure, the grid is uniform in the x-direction, with constant cell width, dx, of 1 cm or 1.2 cm, for the case of coupling at x=7.5 m and x=0 m respectively; after the structure, it is non-uniform, with increasing cell width. In the y-direction, the grid is uniform with dy=1 cm in the whole domain. The total number of cells in x was 1797 and 1422 for the coupling section in, respectively, x=0m and x=7.5m and 249 in y.

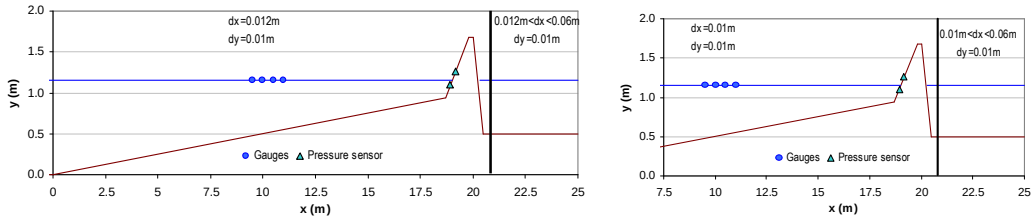

Figure 12: Sketch of the computational grid for the coupling section in x=0 m (left) and in x=7.5 m (right) (axes not scaled).

The numerical tests were run on an Intel(R) Core(TM)2 Quad CPU Q6600 @2.40GHz with 3.00GB of RAM and the average execution time was about 24 h for 100 s simulations.

3.4 SPHysics

The computational domain reproduced the full dimensions of the ramp and the structure. The paddle (piston type) was located 10.0 m before the beginning of the ramp,

instead of 35.7 m in the experimental flume. The numerical paddle did not include dynamic absorption.

For the present numerical simulations, the quadratic kernel [30] was used to determine the interaction between the particles. The fluid was treated as weakly compressible, which allowed the use of an equation of state to determine fluid pressure. The relationship between the pressure and the density was assumed to follow the equation of state. The compressibility was adjusted to slow the speed of sound so that the time step in the model, based on the sound velocity, was reasonable. The predictor-corrector model for time integration was used and variable time step was adopted to ensure the CFL condition. The repulsive boundary condition, developed by Monaghan [23], was applied and prevented a water particle crossing a solid boundary.

Simulations were carried out considering the sub-particle scale – SPS – turbulence model [31].

Particles are usually moved using the XSPH variant due to Monaghan [32], with ε_{XSPH}=0.5 (values ranged between 0 and 1). The method is a correction for the velocity of a particle, which is recalculated taking into account the velocity of that particle and the average velocity of neighboring particles. However, it was shown that, for wave propagation modeling, instabilities appear for $\varepsilon_{XSPH}\neq 0$ and the program crashes. Consequently, ε_{XSPH}=0 was considered in the simulations [33].

The computational domain was constructed using 2690 solid particles and 148600 fluid particles, with a distance between particles of 0.01292 m in the horizontal and vertical directions. Figure 13 presents the full computational domain and a detail of the initial position of particles near the structure. In the figure, positions of particles are represented using an index skipping of 2.

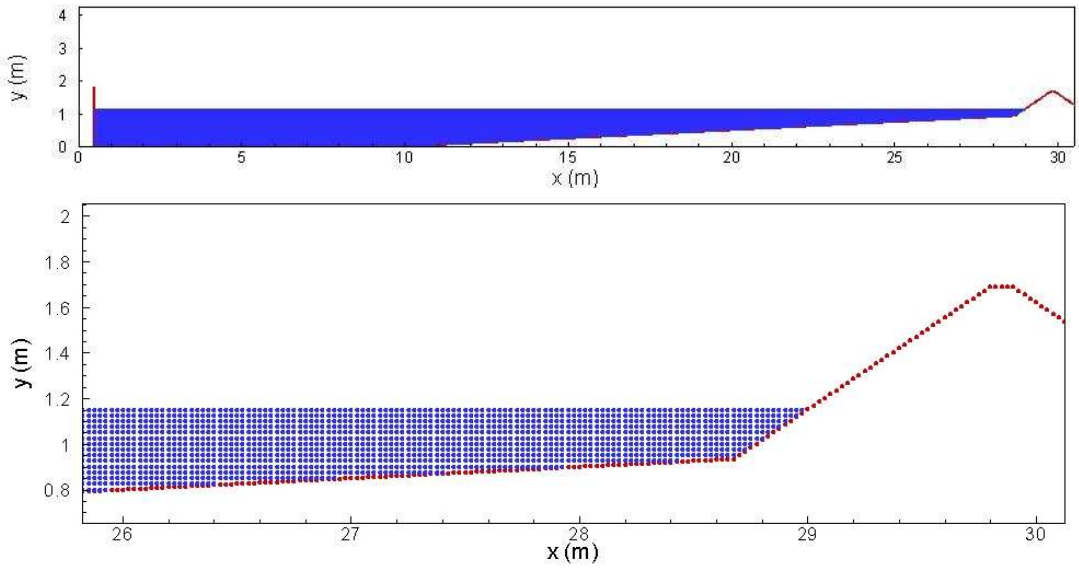

Figure 13: Full computational domain and detail of the initial position of particles near the structure (positions of particles are represented using an index skipping of 2).

Figure 14 shows the free surface elevation at two gauges located at x=7.5 m and x=12.0 m from the beginning of the ramp. There is a good agreement between the numerical results and the experimental data for the two gauges, both in terms of wave amplitude and wave period. However, some differences can be observed that seem probably due to differences in the phase of fundamental frequency and harmonics.

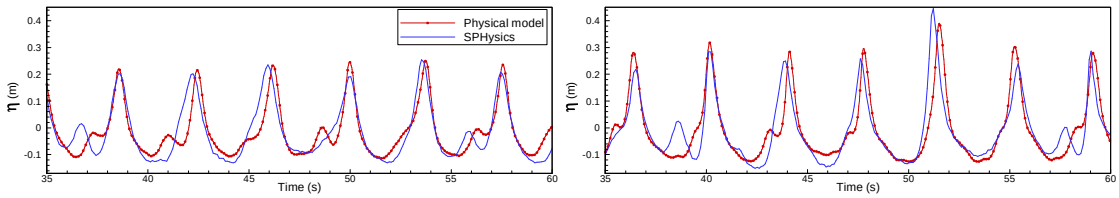

Figure 14: Free surface elevation at gauges located at x=7.5 m and x=12.0 m from the beginning of the ramp.

Figure 15 represents the particle positions at two instants and allows analyzing two types of interaction: wave-wave interaction, between the incident and the reflected waves, and wave-structure interaction, between the incident wave and the coastal structure. In the first case, corresponding to the first figure, wave breaking occurs after the interaction between the incident and the reflected waves, near the coastal structure. In the second case, corresponding to the second figure, run-up is observed on the structure. The wave energy is dissipated and overtopping does not occur.

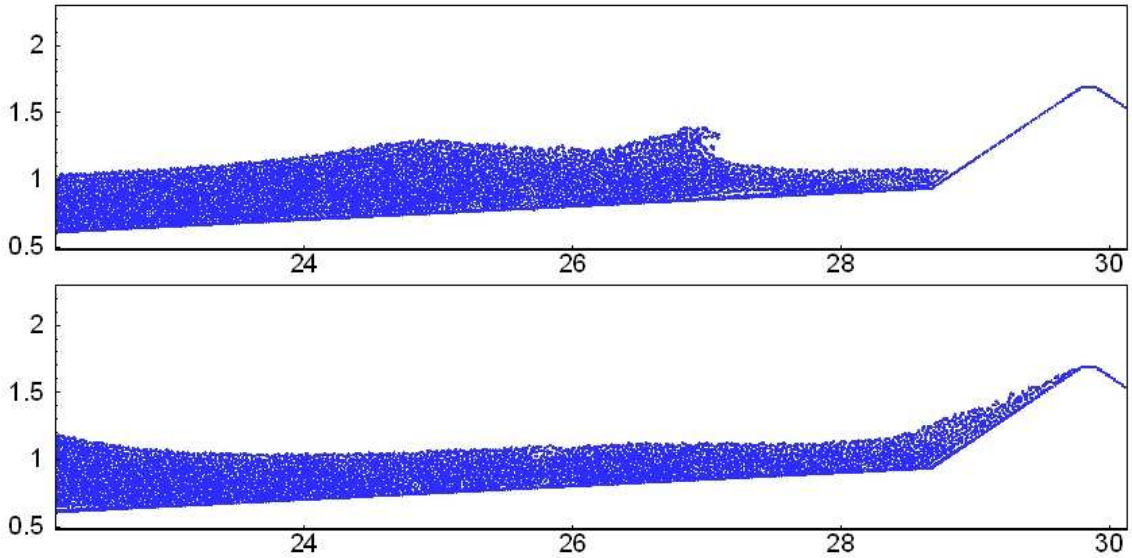

Figure 15: Particles position at two instants.

4 RESULTS AND DISCUSSION

In this section, the results obtained with the three models are compared and discussed. Firstly, the models were run using an input data as similar as possible. Since it is more difficult to impose a certain time series of free surface elevation (and the velocity profiles in the case of COBRAS-UC and SPHysics) in the model SPHysics, it was decided to run SPHysics using a computational domain as defined in section 3.4, with a paddle located 10 m before the beginning of the ramp. The SPHysics results obtained in sections x=0 m and x=7.5 m were used as input for AMAZON (free surface elevation, i.e. incident plus reflected wave series) and for COBRAS-UC (free surface elevation and the two components of the velocity profile).

Additionally, SPHysics and COBRAS-UC were run for the wave condition used as an input condition in the physical model (H=0.40 m, T=3.79 s) and compared with the experimental data. AMAZON was run using as input the incident plus reflected wave series obtained from COBRAS-UC for x=8.5 m. The free surface elevation at x=9.5 m, 10.0 m, 10.5 m and 11.0 m and the mean overtopping discharges computed by the three models are compared to the physical model data at sections 4.1 and 4.2, respectively.

4.1 Surface elevation

The free surface elevation obtained with the three models for the wave condition used in this study is compared wit the measurements made in the physical model at the 4 gauges located at x=9.5 m, 10.0 m, 10.5 m and 11.0 m (Figure 16).

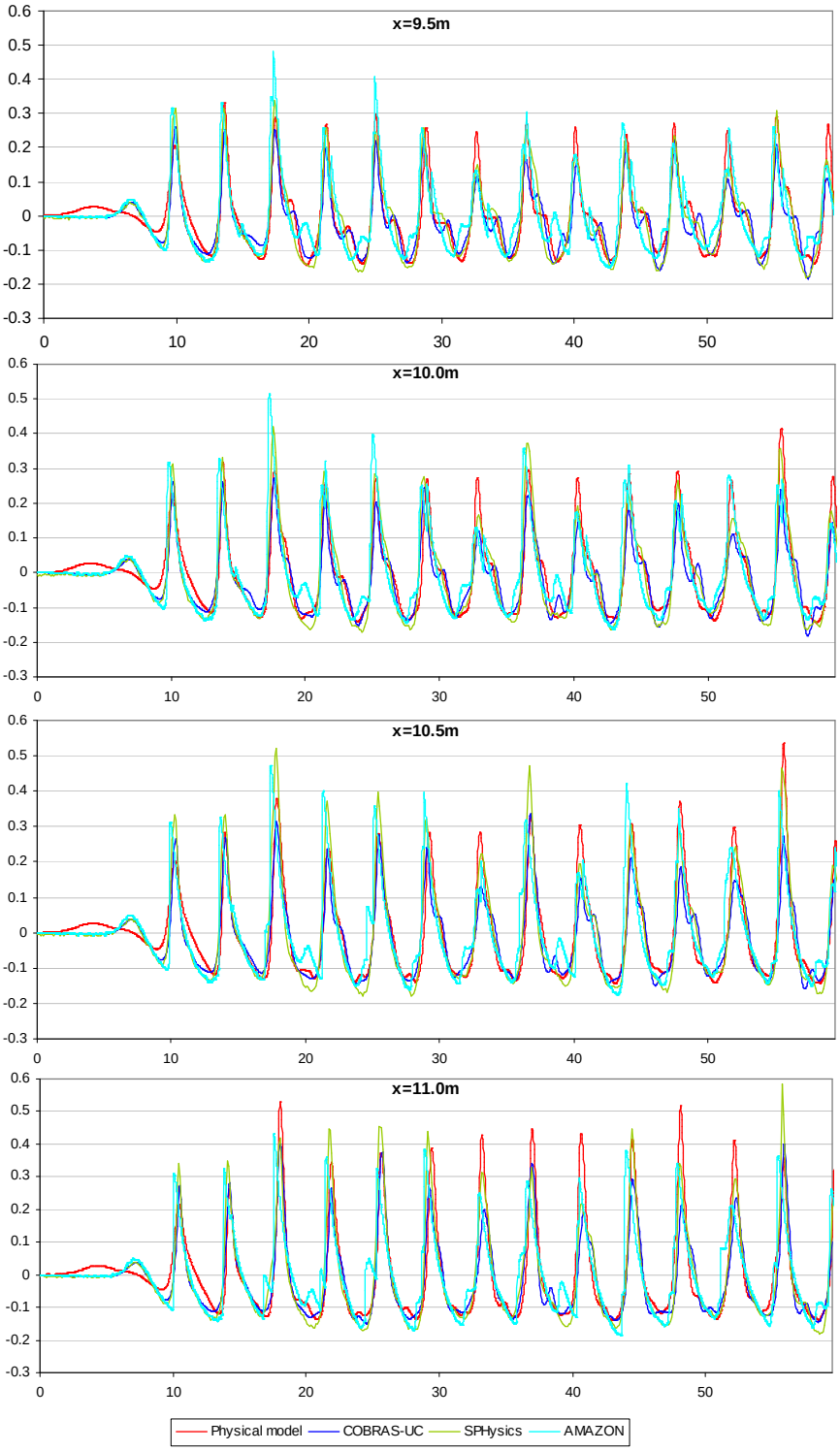

Figure 16: Surface elevation at the four gauges used in the physical model tests.

Although the processes of wave generation used in the laboratory (paddle with wave absorption system) and in the models are different (SPHysics has a paddle without

absorption and AMAZON has used as input data the incident plus reflected wave series from COBRAS-UC at x=0 m), the agreement in the free surface for these four locations is reasonable. The wave period obtained with the models agree very well with the data. The shape of the wave presents some minor differences to the physical model data, as well as the wave height (Table 3 and Figure 17). The maximum difference between the wave height obtained by the models, H, and obtained in the physical model, H_{pm}, is about 17%.

x (m)	-30.8	-30.4	9.5	10.0	10.5	11.0	Max [abs(H-H_{pm})/H_{pm}]
Experimental data, H_{pm}	**0.44**	**0.46**	**0.41**	**0.44**	**0.52**	**0.60**	-
SPHysics	-	-	0.43	0.50	0.60	0.65	15%
COBRAS-UC	0.49	0.50	0.42	0.46	0.55	0.63	10%
AMAZON	-	-	0.46	0.52	0.58	0.54	17%

Table 3 – Wave height, Hs, obtained with the models and experimental data

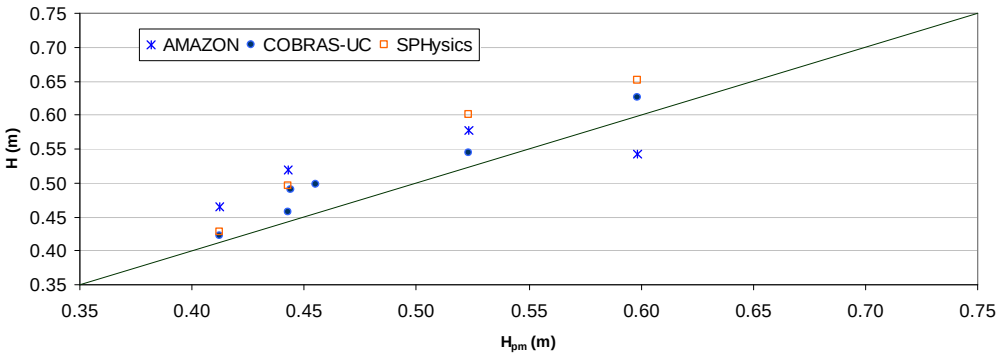

Figure 17: Wave height (H) obtained with the different models and obtained in the physical model tests (H_{pm}).

4.2 Wave overtopping discharge

The mean overtopping discharges computed by the three models with different coupling options but with similar input data, the SPHysics results at x=0 m and x=7.5 m, are compared (Figure 18). In order to avoid the influence on the results of the re-reflected waves from the paddle, the mean overtopping discharges presented correspond to the values that occur between the 2nd and the 7th waves that reach the structure. Only as a reference, the results are also compared with the range of values obtained in the physical model.

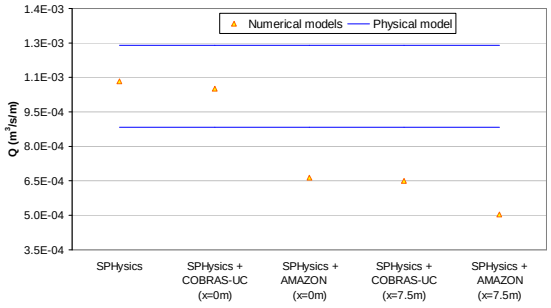

Model	Coupling section	Q (m³/s/m)
SPHysics	-	1.08E-03
SPHysics + COBRAS-UC	x=0.0m	1.05E-03
SPHysics + AMAZON		6.65E-04
SPHysics + COBRAS-UC	x=7.5m	6.48E-04
SPHysics + AMAZON		5.05E-04
Physical model	-	8.85E-4 to 1.24E-3

Figure 18: Mean overtopping discharges obtained with the different coupling options but with similar input data.

As can be seen in the figure, the results obtained with SPHysics and COBRAS-UC for x=0 m agree very well. However, AMAZON, where the information of the velocity profile was not introduced, gives a lower value of Q. Moreover, the input of AMAZON includes the incident and the reflected waves. The results suggest that, even before the ramp starts, the influence of the reflected wave is important and the fact that this information is not introduced, by using only the incident wave as input or the velocity profile, has a significant influence on the final value of Q.

For x=7.5 m both the COBRAS-UC and the AMAZON models give lower values of Q than SPHysics. As the overtopping is very sensitive to the height and shape of the wave, one explanation for these results may be that SPHysics reduces the wave height during propagation giving lower values of the wave height at this section, located in the ramp, leading to a reduction in the values of Q. Another reason may be that more energetic harmonics are present at x=7.5 m due to reflection and propagation than at x=0 m. When used as input of the other models, small errors in the phase of each harmonic can lead to important differences in the final mean overtopping discharge, even for cases where the impact on the surface elevation is small. This case study is especially difficult to be modeled since a small modification on the wave height and shape can lead to a different breaking position and/or position of the incident and reflected wave interaction, influencing the obtained mean overtopping discharge.

Additionally, the mean overtopping discharges computed by the three models for the test conditions considered in this study (H=0.40 m, T=3.79 s), are compared with the range of values obtained in the physical model. As explained in section 3.2, AMAZON uses as input the incident plus the reflected wave series from COBRAS-UC at x=8.5 m. Figure 19 summarizes the main results obtained.

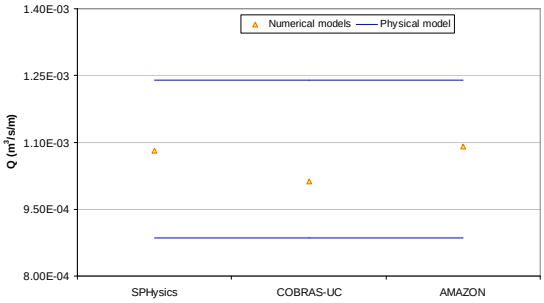

Model	Q (m^3/s/m)
SPHysics	1.08E-03
COBRAS-UC	1.01E-03
AMAZON	1.09E-03
Physical model	8.85E-4 to 1.24E-3

Figure 19: Mean overtopping discharges obtained with the three models.

As can be seen in the figure, the results obtained by the three models agree very well with the physical model results.

5 CONCLUSIONS

This paper compares the output from three numerical models used to predict the mean overtopping discharges: AMAZON [1], based on solving the non-linear shallow-water equations; and two models based on Reynolds averaged Navier-Stokes equations, COBRAS-UC [2], a Eulerian model using the volume of fluid (VoF) method for surface capturing, and SPHysics [3], a Lagrangian model based on Smoothed Particle Hydrodynamics (SPH). The numerical results are also compared with experimental data collected at the National Civil Engineering Laboratory (LNEC), Portugal, using a 1:10 geometrical scale and consisting of wave propagation, with breaking, and wave overtopping of an impermeable seawall [4].

In order to compare the results obtained with the three models, they were firstly run using similar input data from SPHysics in two different sections: one located at the beginning of the ramp, about 18 m from the structure, and another located at the ramp, 7.5 m from the first section. Previously, a sensibility analysis of the impact on the results of the position of the input section and of the mesh refinement was performed for AMAZON and for COBRAS-UC in order to define the computational domain and the mesh refinement to be used to run the models. The results of mean overtopping discharges obtained with SPHysics and COBRAS-UC for the first section agreed very well. However, AMAZON, where the information of the velocity profile was not introduced, gave a lower value of Q. Moreover, the input of AMAZON included the incident and the reflected waves. The results suggested that, even before the ramp starts, the influence of the reflected wave was important and the fact that this information was not introduced in AMAZON, by using only the incident wave as input or the velocity profile, had a significant influence on the final value of Q. For the second section, both the COBRAS-UC and the AMAZON models gave lower values of Q than SPHysics. One explanation for these results may be that SPHysics reduces the wave height during propagation giving lower values of the wave height at this section leading to a reduction in the values of Q. Summarizing, when coupling models, the position of the coupling section and the data transferred between the models have a significant influence on the final results, especially on the mean overtopping discharge obtained.

Additionally, the models were run for the test conditions considered in this study (H=0.40 m, T=3.79 s). The free surface elevation at four positions and the mean overtopping discharges were compared with the physical model data. Although the processes of wave generation used in the laboratory and in the models were different, the agreement in the free surface for the four locations was reasonable: the wave period obtained with the models agreed very well with the data and the shape of the wave presented some minor differences to the physical model data, as well as the wave height. The results of mean overtopping discharges obtained with the three models agreed very well with the physical model results.

Note that this case study is especially difficult to be modeled since a small modification on the wave height and on the shape of the wave can lead to a different breaking position and/or position of the incident and reflected wave interaction and, consequently, to different mean overtopping discharge.

ACKNOWLEDGMENTS

The authors gratefully acknowledge the financial support of the HYDRALAB III Project, which is an Integrated Infrastructure Initiative within the Research Infrastructures Program of FP6, Contract N. 022441.

REFERENCES

[1] M.T. Reis, K. Hu, M.G. Neves and T.S. Hedges, Numerical modelling of breakwater overtopping using a NLSW equation model with a porous layer, In proceedings of the *31st ICCE*, Hamburg, Germany, August 31 to September 5, 2008, J.M. Smith (Ed.), World Scientific, Singapore, 2009, pp. 3097-3109 (2008)

[2] I.J. Losada, J.L. Lara, R. Guanche and J.M. Gonzalez-Ondina, Numerical analysis of wave overtopping of rubble mound breakwaters, *Coastal Engineering*, **55**(1), pp. 47-62 (2008)

[3] A.J.C. Crespo, M. Gómez-Gesteira and R.A. Dalrymple, Modeling dam break behavior over a wet bed by a SPH technique, *Journal of Waterway, Port, Costal, and Ocean Engineering*, **134**(6), pp. 313-320 (2008)

[4] M.T. Reis, M.G. Neves and C.J. Fortes, Influence of physical model scale in the simulation of wave overtopping over a coastal structure, In proceedings of the *PIANC Mediterranean Days of Coastal and Port Engineering*, Palermo, Italy, October 7-9, PIANC (2008)

[5] T.-J. Hsu, T. Sakakiyama and P.L.-F. Liu, A numerical model for wave motions and turbulence flows in front of a composite breakwater, *Coastal Engineering*, **46**, pp. 25-50 (2002)

[6] A. Kortenhaus, H. Oumeraci, J. Geeraerts, J. de Rouck, J.R. Medina and J.A. González-Escrivá, Laboratory effects and further uncertainties associated with wave overtopping measurements, In proceedings of the *29th ICCE*, Lisbon, Portugal, September 19-24, 2004, J.M. Smith (Ed.), World Scientific, Singapore, 2005, pp. 4456-4468 (2004)

[7] J.L. Lara, N. Garcia and I.J. Losada, RANS modelling applied to random wave interaction with submerged permeable structures, *Coastal Engineering*, **53**, pp. 395-417 (2006)

[8] D. Ingram, D. Causon, C. Mingham and J.G. Zhou, Numerical simulation of violent wave overtopping, In proceedings of the *28th ICCE*, Cardiff, July 7-12, 2002, J.M. Smith (Ed.), World Scientific, Singapore, 2003, pp. 2286-2298 (2002)

[9] D.M. Ingram, D.M. Causon, F. Gao, C.G. Mingham, P. Troch, T. Li and J. De Rouck, *Free Surface Numerical Modelling of Wave Interactions with Coastal Structures*, CLASH WP5 – Report, Manchester Metropolitan University and University of Gent (2004)

[10] S. Shao, C. Ji, D.I. Gram, D.E. Reeve, P.W. James and A.J. Chadwick, Simulation of wave overtopping by an imcompressible SPH model, *Coastal Engineering*, **53**, pp. 723-725 (2006)

[11] K. Hu, *High-Resolution Finite Volume Methods for Hydraulic Flow Modelling*, PhD Thesis, Centre for Mathematical Modelling and Flow Analysis, Manchester Metropolitan University, UK (2000)

[12] A.J.C. Crespo, *Application of the Smoothed Particle Hydrodynamics model SPHysics to Free-Surface Hydrodynamics*, PhD Thesis, University of Vigo, Spain (2008)

[13] K. Hu and D. Meyer, The validity of the non-linear shallow water equations for modelling wave runup and reflection, In proceedings of the *ICE Coastlines, Structures & Breakwaters '05*, Thomas Telford, pp. 195-206 (2005)

[14] M. Gómez-Gesteira, R.A. Dalrymple, A.J.C. Crespo and D. Cerqueiro, Uso de la técnica SPH para el estúdio de la interacción entre olas y estructuras, *Ingenieria del Água*, **11**(2), pp. 147-170 (2004)

[15] R.A. Dalrymple and B.D. Rogers, Numerical modeling of water waves with the SPH method, *Coastal Engineering*, **53**(2-3), pp. 141-147 (2006)

[16] M.T. Reis, M.G. Neves and K. Hu, Wave overtopping of a porous structure: numerical and physical modelling, *Journal of Coastal Research*, SI **56**, pp. 539-543 (2009)

[17] M.T. Reis, M.G. Neves, K. Hu, M.R. Lopes and L.G. Silva, Final rehabilitation of Sines west breakwater: physical and numerical modelling of overtopping, In proceedings of the *Coasts, Marine Structures and Breakwaters 2009*, Edinburgh, Scotland, September 16-18, ICE (2009) - in press

[18] M.T. Reis, M.G. Neves, M.R. Lopes and L.G. Silva, Overtopping physical model tests for the rehabilitation of Sines west breakwater, In proceedings of the *PIANC MMX Congress*, Liverpool, May 10-14 (2010)

[19] P. Lin and P.L.-F. Liu, A numerical study of breaking waves in the surf zone, *Journal of Fluid Mechanics*, **359**, pp. 239-264 (1998)

[20] N. Garcia, J.L. Lara and I.J. Losada, 2-D Numerical analysis of near-field flow at low-crested permeable breakwaters, *Coastal Engineering*, **51**, pp. 991-1020 (2004)

[21] L.B. Lucy, A numerical approach to the testing of the fission hypothesis, *Astron. J.*, **82**(12), pp. 1013-1024 (1977)

[22] A. Gingold and J.J. Monaghan, Smoothed particle hydrodynamics: theory and application to non-spherical stars, *Monthly Notices of the Royal Astronomical Society*, **181**, pp. 375-389 (1977)

[23] J.J. Monaghan, Simulating free surface flows with SPH, *Journal of Computational Physics*, **110**, pp. 399-406 (1994)

[24] R.A. Dalrymple, O. Knio, D.T. Cox, M. Gómez-Gesteira and S. Zou, Using Lagrangian particle method for deck overtopping, In proceedings of the *Waves ASCE*, pp. 1082-1091 (2001)

[25] SPHysics code v1.4, http://wiki.manchester.ac.uk/sphysics

[26] J.J. Monaghan, Smoothed Particle Hydrodynamics, *Annual Review of Astronomy and Astrophysics*, **30**, pp. 543-574 (1992)

[27] C. Fortes, M.G. Neves, J.A. Santos, R. Capitão, A. Palha, R. Lemos, L. Pinheiro and I. Sousa, A methodology for the analysis of physical model scale effects on the simulation of wave propagation up to wave breaking. Preliminary physical model results, In proceedings of the *OMAE 2008*, ASME, No. 57767 (2008)

[28] P. Troch, *User Manual: Active Wave Absorption System*, Gent University, Department of Civil Engineering, Denmark (2005)

[29] T. Pullen and N.W.H. Allsop, *Use of Numerical Models of Wave Overtopping: A Summary of Current Understanding*, Homepage of HR Wallingford, Online, available: http://www.hrwallingford.co.uk/downloads/ projects/overtopping/num model guidance.pdf [2010-03-26] (2003).

[30] G.R. Liu and M.B. Liu, *Smoothed Particle Hydrodynamics: a mesh free particle method*, World Scientific (2003)

[31] H. Gotoh, T. Shibahara and T. Sakai, Sub-particle-scale turbulence model for the MPS method – Lagrangian flow model for hydraulic engineering, *Computational Fluid Dynamics Journal*, **9**(4), pp. 339-347 (2001)

[32] J.J. Monaghan, On the problem of penetration in particle methods, *Journal of Computational Physics*, **82**, pp. 1-15 (1989)

[33] E. Didier and M.G. Neves, Coastal flow simulation using SPH: Wave overtopping on an impermeable coastal structure, In proceedings of the *4th International SPHERIC workshop*, Nante, France (2009)